Surface-Assisted Formation, Assembly, and Dynamics of Planar Organometallic Macrocycles and Zigzag Shaped Polymer Chains with C—Cu—C Bonds

Qitang Fan,[†] Cici Wang,[†] Yong Han,[†] Junfa Zhu,[†,*] Julian Kuttner,[‡] Gerhard Hilt,[‡] and J. Michael Gottfried[‡,*]

[†]National Synchrotron Radiation Laboratory and Collaborative Innovation Center of Suzhou Nano Science and Technology, University of Science and Technology of China, Hefei 230029, P.R. China and [‡]Fachbereich Chemie, Philipps-Universität Marburg, Hans-Meerwein-Strasse, 35032 Marburg, Germany

ABSTRACT The formation, structure, and dynamics of planar organometallic macrocycles (*meta*-terphenyl-Cu)$_n$ and zigzag-shaped one-dimensional organometallic polymers on a Cu(111) surface were studied with scanning tunneling microscopy (STM) and X-ray photoelectron spectroscopy (XPS). Vapor deposition of 4,4″-dibromo-*meta*-terphenyl (DMTP) onto Cu(111) at 300 K leads to C—Br bond scission and formation of C—Cu—C bonds, which connect neighboring *meta*-terphenyl fragments such that room-temperature stable macrocycles and zigzag chains are formed. The chains self-assemble to form islands, which are elongated in the direction of the chains. If DMTP is deposited onto Cu(111) held at 440 K, the island size is drastically increased (>200 × 200 nm^2). STM sequences show the formation of ordered structures through reversible scission and reformation of the C—Cu—C bonds. The cyclic organometallic species such as the hexamer (*meta*-terphenyl-Cu)$_6$ may represent intermediates in the surface-confined Ullmann synthesis of hydrocarbon macrocycles such as the recently discovered hyperbenzene.

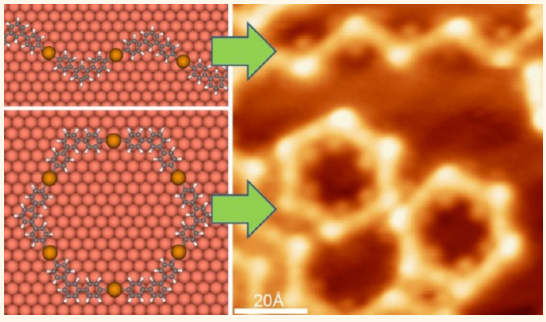

KEYWORDS: scanning probe microscopy · photoelectron spectroscopy · Ullmann reaction · surface chemistry · organometallic chemistry · hyperbenzene · copper

During the past two decades, numerous examples for the controlled bottom-up fabrication of surface nanostructures have been reported, which have great potential for applications in molecular electronics, catalysis, gas storage, magnetism and other fields.[1−4] Especially one- and two-dimensional (1D/2D) organometallic and coordination polymers have attracted attention, because they are often thermally more stable[5−7] than structures based on the weaker electrostatic interactions[8,9] or hydrogen bonds.[10] Compared to covalent linkage,[11] coordination and organometallic bonds have the advantage that bond formation is reversible, and therefore, defects in the translational symmetry can heal through bond scission and reformation. Most previous 2D supramolecular coordination polymers and nanostructures were based on organic ligands with linkers such as pyridyl,[5,12,13] carboxylate,[14,15] carbonitrile[16] or biphenol.[16] Related organometallic systems with carbon—metal—carbon bonds have also been reported, partly as potential intermediates in the surface-assisted Ullmann reaction[17,18] for the synthesis of 1D and 2D covalent nanostructures.[19−23]

To control the formation and the final topography of the surface-confined organometallic and coordination nanostructures at the atomic level, it is necessary to understand the factors that influence the self-assembly, *e.g.*, the structural relations between precursor and substrate, bond strength and reversibility of bond formation, as well as precursor mobility and availability. For example, formation of the desired nanostructures is facilitated by structurally matching combinations of precursor and substrate, which highlights the significance of commensurability between the formed structure and the substrate lattice.[13,16,24,25] The type of the metal center can also greatly influence the structures of the organometallic or coordination networks.[7,13] In addition,

* Address correspondence to jfzhu@ustc.edu.cn, michael.gottfried@chemie.uni-marburg.de.

Received for review October 15, 2013 and accepted December 11, 2013.

Published online December 11, 2013
10.1021/nn405370s

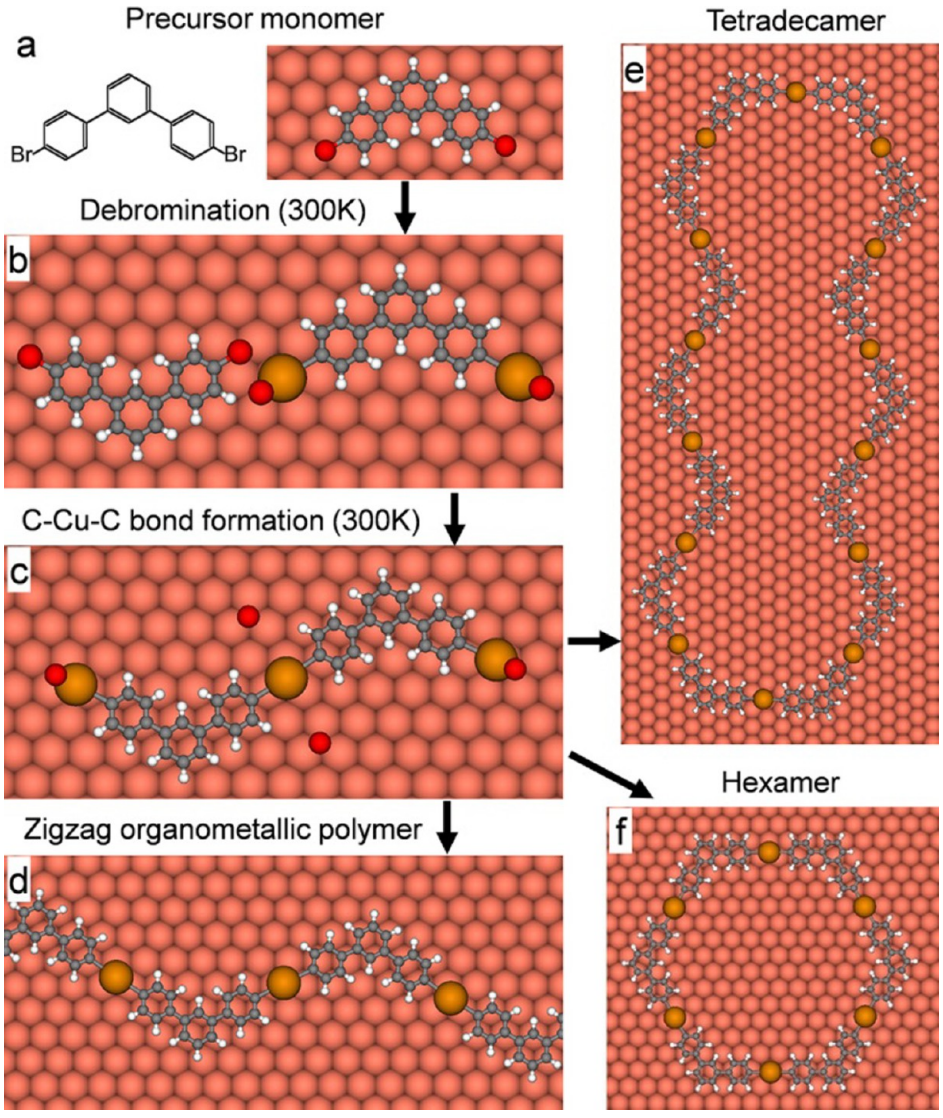

Figure 1. Reactions of (a) 4,4″-dibromo-*meta*-terphenyl (DMTP) 1 on Cu(111). (b) Scission of the C−Br bond and insertion of a Cu atom presumably leads to (c) an intermediate which can form (d) organometallic polymer chains 2 or (e and f) macrocyclic organometallic oligomers. Color code: white, hydrogen; gray, carbon; red, bromine; underlying Cu(111) surface atoms are shown by orange spheres.

the abundance of the substrate-provided metal atoms is expected to affect the formation of the surface nanostructures, but has not found much attention previously. Because of the restriction of substrate commensurability and the selected ligands, only few 1D straight organometallic and coordination polymers have been reported,[6,19,24,26−30] none of which did arrange into large islands of well-ordered structure.

In this work, we report the surface-assisted synthesis of stable planar organometallic macrocycles and 1D polymers from 4,4″-dibromo-*meta*-terphenyl **1** (DMTP). The structures of the precursor and some of the products are shown in Figure 1. The precursor **1** was chosen because its internal angle of 120° allows folding of the chains and formation of macrocycles. The 120° angle also matches the symmetry of the Cu(111) substrate, which thus may provide additional stabilization.[16] We will show that the polymer **2** forms zigzag chains (Figure 1d) and macrocycles such as (*meta*-terphenyl-Cu)$_6$ or (*meta*-terphenyl-Cu)$_{14}$ (Figure 1e,f), in which *meta*-terphenyl fragments are linked by linear C−Cu−C bonds.

Reactions of bromoarenes with metallic Cu, first described by Ullmann and Bielicki in 1901, have been widely used for C−C coupling between aromatic rings in solution.[17] Because of the complex nature of the metal/solution interface, a complete mechanistic understanding of this reaction in solution has not been achieved so far. Since the here described organometallic compounds with C−Cu−C bonds represent possible intermediates in the Ullmann reaction, our study gives insight into its mechanism without the interference of solvents. On a wider scope, the bromoarene/Cu interface serves as a prototype for interfaces between

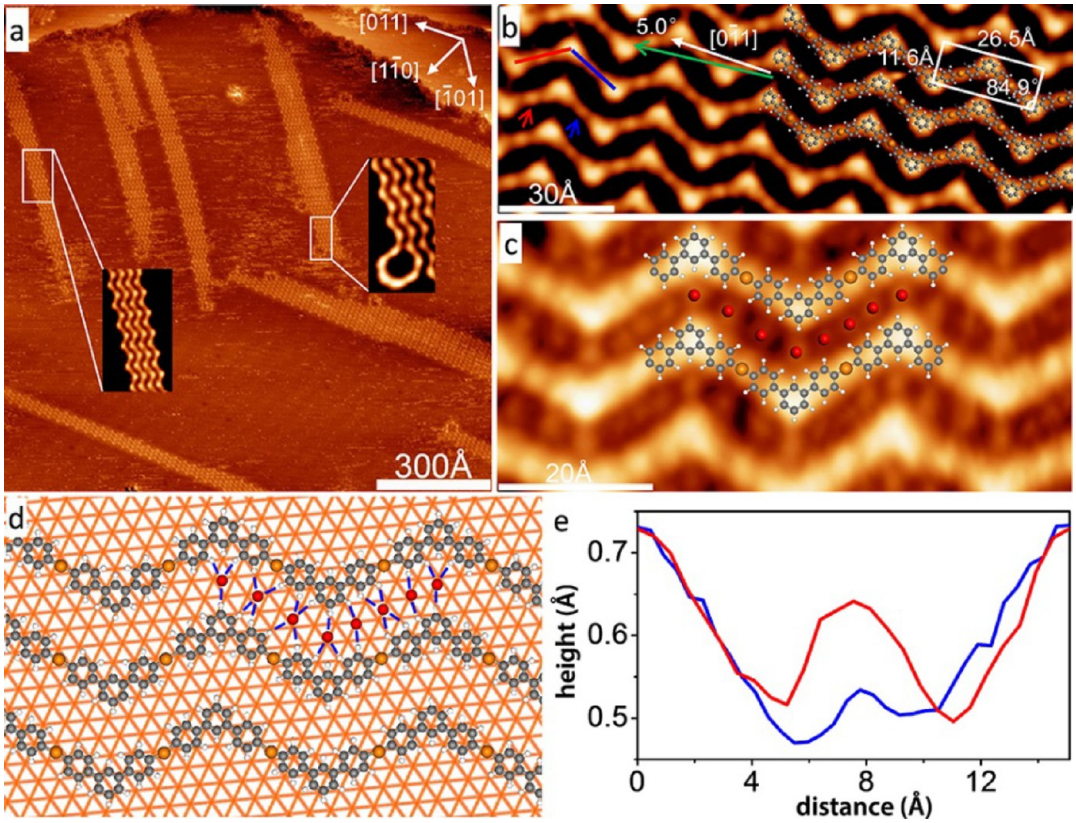

Figure 2. STM images of the organometallic polymers with C−Cu−C bonds on Cu(111). (a) Overview STM image after deposition of 0.22 ML DMTP 1 at 300 K; tunneling parameters $U = -2.75$ V, $I = 0.03$ nA. (b) High-resolution image of an island of the organometallic polymer 2 with overlaid molecular model and unit cell; the angle of 5.0° between chain direction (green arrow) and [0$\bar{1}$1] direction (white arrow) is displayed; $U = -3.6$ V, $I = 0.01$ nA; imaging at a sample temperature of 90 K. (c) High-resolution STM image showing Br atoms between the chains; $U = -3.2$ V, $I = 0.07$ nA; imaging at 90 K. Selected Br atoms are marked with red discs. (d) Tentative model of 2 on a Cu(111) surface lattice with approximate positions of the Br atoms. Color code: C, gray; H, white; Br, red; Cu and Cu(111) lattice, orange. Possible H bridge bonds are marked by blue lines. (e) Apparent height profile along the red and blue lines in (b) from bottom to top (average over five symmetry equivalent lines).

metals and haloarenes; its investigation thus contributes to the general understanding of elementary steps of heterogeneous reactions in organic and organometallic synthesis.

RESULTS

Figure 1 illustrates possible reactions of 4,4″-dibromo-*meta*-terphenyl (DMTP) **1** on Cu(111). According to previous studies using other aromatic halides,[19,28,31] deposition of DMTP (Figure 1a) onto Cu(111) at 300 K likely leads to scission of the C−Br bonds and formation of a *meta*-terphenyl fragment. In the gas phase, this species would be a biradical, but on the surface, the radical C atoms are most likely saturated by Cu adatoms. Another possibility is insertion of Cu into the C−Br bond, resulting in an organometallic intermediate with C−Cu−Br end groups. Formation of C−Cu−C bonds between the intermediates leads to chains (Figure 1d) or cyclic species (Figure 1e,f).

Figure 2a shows an STM image taken after deposition of 0.22 ML DMTP **1** onto Cu(111) held at 300 K. The elongated, stripe-like islands consist of zigzag chains of the organometallic polymer **2**. Most islands have a large length/width ratio of up to 25:1, which suggests that adding another *meta*-terphenyl fragment to an existing chain is much faster than the start of a new chain.

Statistical analysis of the orientation of the chains relative to the substrate reveals that only six directions occur, with angles of ±5.0° relative to the substrate high symmetry directions ([0$\bar{1}$0] and equivalent). These orientations apparently ensure optimal registry with the substrate, as will be examined further in the Discussion section. Figure 2b shows a selected area of an island at higher magnification. Each 120° bent of a chain represents a single *meta*-terphenyl fragment. The brightest protrusions along the chain are the central phenyl rings. The bridging Cu atoms appear as weak protrusions in the center of the straight parts of the chains. The unit cell of the island structure (ignoring the influence of the substrate symmetry) is also displayed in Figure 2b. The length of the repeat unit along the chains (26.5 Å) is consistent with the presence of a Cu atom between the *meta*-terphenyl fragments, because direct C−C linkage would result in a shorter repeat unit of only 21.8 Å, see ref 22. The large

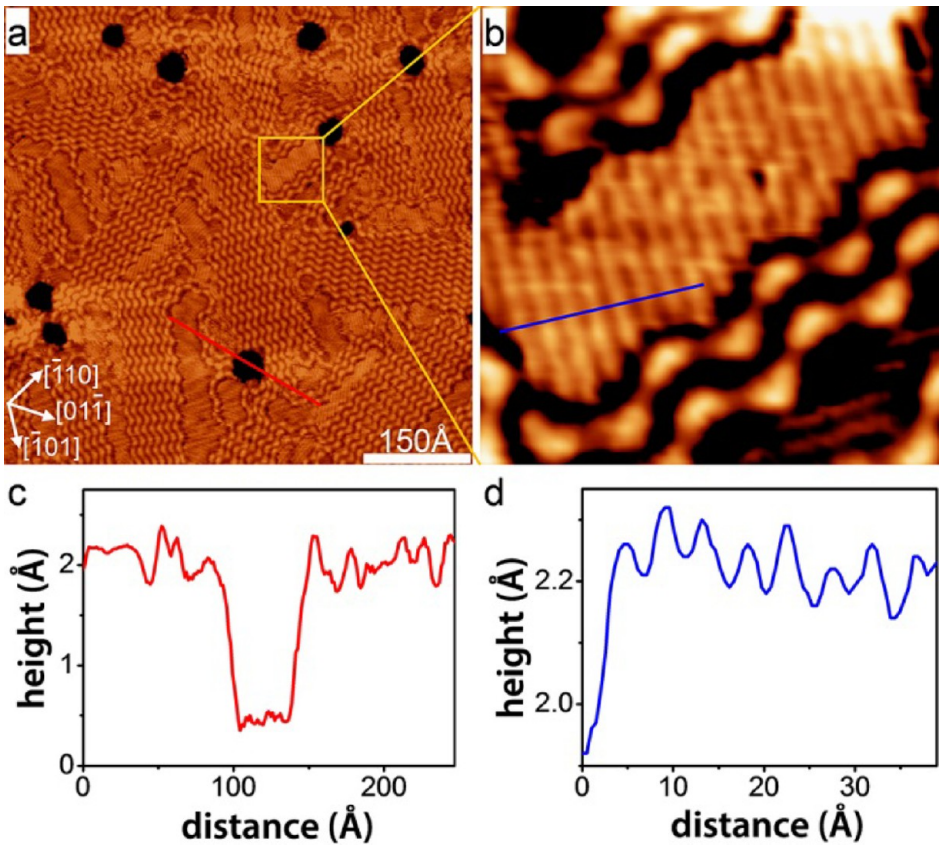

Figure 3. STM images recorded after deposition of DMTP at 300 K using higher coverages than those used in Figure 2: (a) 0.77 ML organometallic polymer 2 prepared at 300 K, $U = -2.75$ V, $I = 0.03$ nA; (b) magnified view of framed area in (a), $U = -2.75$ V, $I = 0.05$ nA; (c) apparent height profile along the red line in (a) from top to bottom; (d) apparent height profile along the blue line in (b) from left to right.

lattice constant perpendicular to the chains (11.6 Å) shows the absence of covalent bonds between the chains. The islands are frequently terminated by a step edge on the one end and by the encounter with another island on the other end. Island growth along the chains is also interrupted by the backfolding of chains, as can be seen in Figure 2a (right inset): the chain forms a loop at the end of the island and continues in the opposite direction. This near-hexagonal loop is the smallest and thus most rigid loop that can be formed with the 120° angles of the precursor molecule. Larger loops could be more flexible and move during imaging; their existence could explain why the "open" ends of islands often appear fuzzy in STM. Figure 2c, taken at 90 K, shows a section of an island at even higher magnification and different contrast. The spot-like protrusions between the chains are assigned to chemisorbed Br atoms, in agreement with the literature.[19,28] Evidence for the presence of adsorbed Br atoms resulting from C−Br bond scission is provided by the X-ray photoelectron spectra in Figure S1 in the Supporting Information. However, due to the general lack of local, chemically sensitive probes, it cannot be completely excluded that the protrusions between the chains are related to Cu atoms. More details are presented in the Supporting Information.

Deposition of higher (but still submonolayer) coverages of DMTP does not lead to increased island sizes, even though deposition rates as low as 0.022 ML/min were applied in order to maintain near-equilibrium growth conditions. As shown in Figure 3a, the islands are shorter along the direction of the chains, apparently because they have less space to grow before colliding with another island. In addition, dark features (holes) appear on the Cu(111) surface. Their depth of 1.8 Å (see the line scan in Figure 3c) agrees with the height of a monatomic step, which is 1.9 Å.[32] This suggests that the holes represent vacancy islands of missing Cu atoms, which are probably incorporated in the C−Cu−C bonds, as will be considered in the Discussion section.

Between the islands of the organometallic chains, Figure 3a shows areas with an ordered row-like structure, which is displayed with higher magnification in Figure 3b. According to the line scan in Figure 3d, the distance between two neighboring rows is 4.5 Å, *i.e.*, $\sqrt{3}$ times the distance between two neighboring Cu atoms. These features are tentatively assigned to islands of Br adatoms (see above); more details are presented in the Discussion section and in the Supporting Information.

Besides the zigzag chains, cyclic oligomers are observed (Figure 4). In Figure 4b, a cluster of three

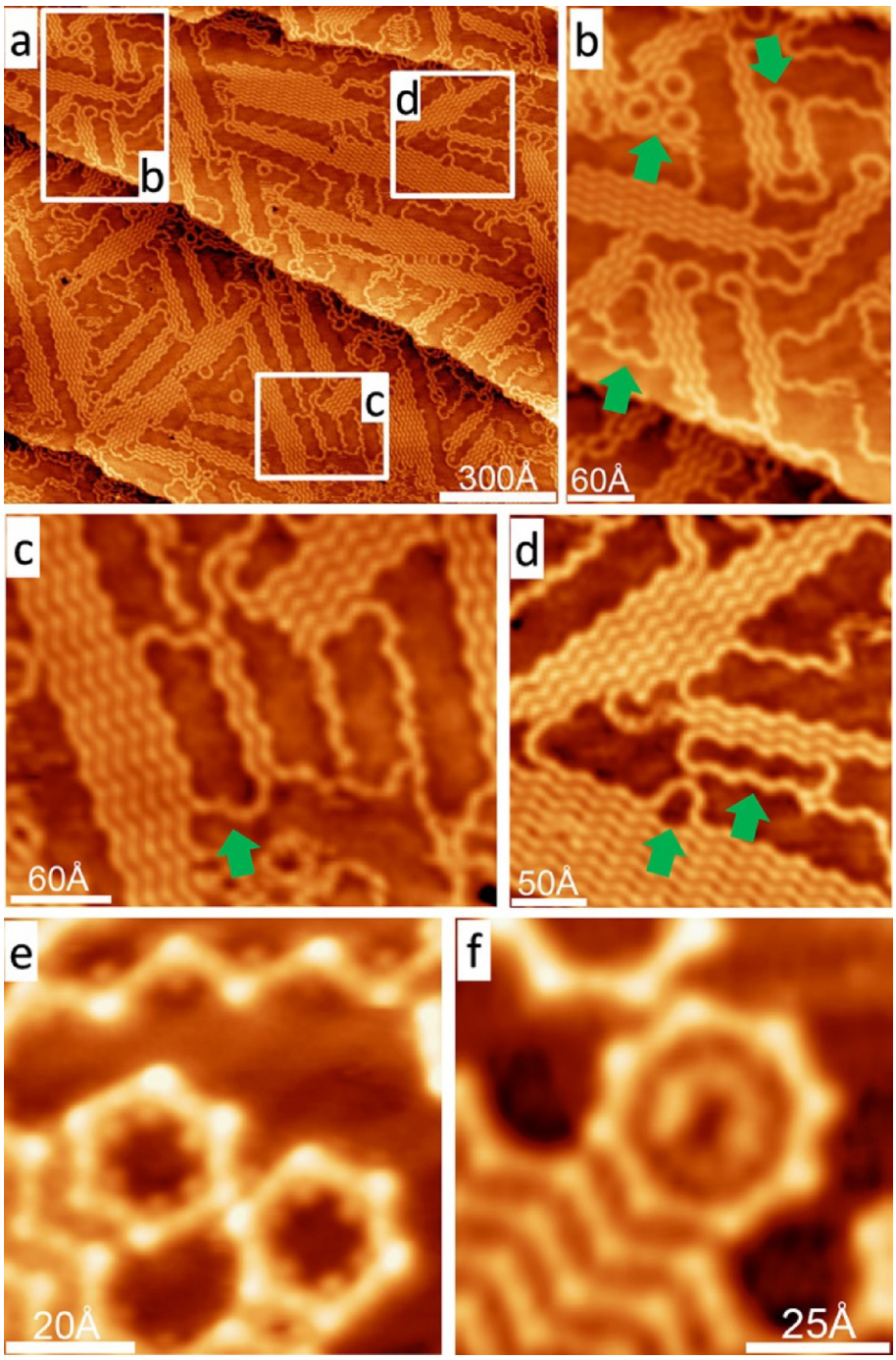

Figure 4. STM images of the organometallic oligomers and polymers at a coverage of 0.55 ML, $U = -2.75$ V, $I = 0.08$ nA: (a) overview STM image; (b) enlarged region of (a) with the macrocycles $(MTP\text{-}Cu)_6$, $(MTP\text{-}Cu)_{14}$ and $(MTP\text{-}Cu)_{16}$, as marked by green arrows, and folded chains; (c) enlarged region of (a) with $(MTP\text{-}Cu)_{22}$ (green arrow); (d) enlarged region of (a) with the macrocycle $(MTP\text{-}Cu)_{18}$ and with an attached chain forming a loop (marked by green arrows); (e) STM image taken after deposition of DMTP onto Cu(111) at 300 K (0.77 ML) and subsequent STM imaging at 90 K, $U = -3.2$ V, $I = 0.06$ nA. Note the Br atoms at the bents of the chains and organometallic hexamers. (f) Macrocycle $(MTP\text{-}Cu)_8$ with inclusions, $U = -3.2$ V, $I = 0.03$ nA.

adjacent hexagons (*meta*-terphenyl-$Cu)_6$ occurs in the upper left part. The presence of linking Cu atoms is supported by the fact that this hexamer has a diameter of 25.2 Å, which exceeds the diameter of 21.3 Å found for the respective hydrocarbon macrocycle without Cu atoms, hyperbenzene.[22] On the right-hand side of Figure 4b, a macrocycle with 14 *meta*-terphenyl (MTP) units, $(MTP\text{-}Cu)_{14}$, and in the lower part a hexadecamer $(MTP\text{-}Cu)_{16}$ can be seen. Panes c and d of Figure 4 show the macrocycles $(MTP\text{-}Cu)_{22}$ and $(MTP\text{-}Cu)_{18}$, respectively. In the room-temperature images in Figure 4a–d, almost all cyclic species are partly embedded by chains. This seems necessary for the stabilization of the rings. It is not surprising that the rings are less stable than

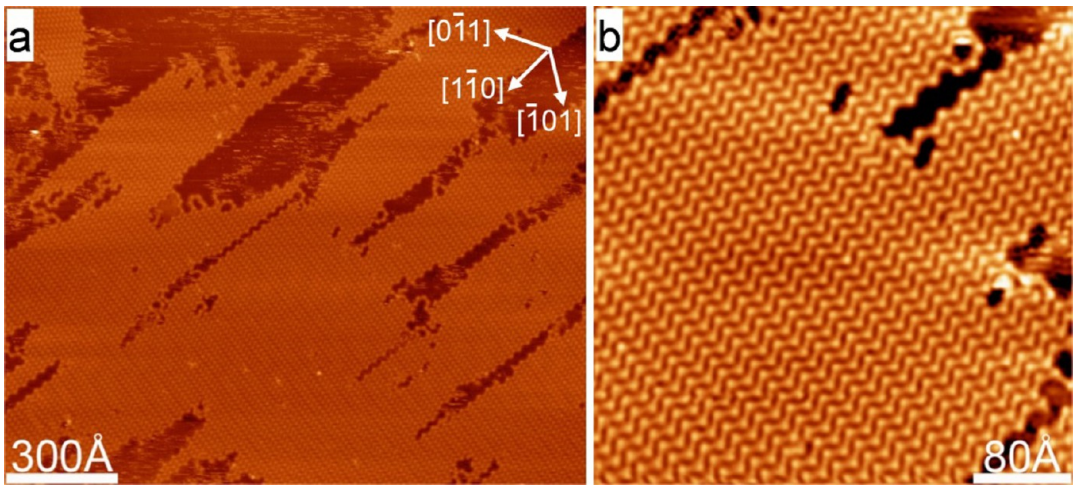

Figure 5. (a) STM images of large islands of the organometallic polymer 2 obtained by deposition of 0.77 ML DMTP 1 onto Cu(111) held at 440 K; $U = -3.6$ V, $I = 0.01$ nA. (b) Magnified image of the central area in (a), $U = -3.6$ V, $I = 0.02$ nA.

(islands of) chains, because the higher packing density of the chains increases mutual stabilization by van der Waals interactions (see Discussion). This would also explain why the macrocycles rarely occur in the low-coverage images (Figure 2). The lower stability makes it also more difficult to image the macrocycles at room temperature using smaller tip−sample distances without destroying them; in contrast, islands of chains are significantly more stable. Imaging of macrocycles at 90 K proved to be more successful, as shown in Figure 4e, in which two separate rings occur next to an isolated chain. Figure 4f shows an octamer $(MTP\text{-}Cu)_8$. Its octagonal structure requires internal angles of 135°, which are larger than 120° and thus not favored by the structures of substrate and precursor. This ring is probably stabilized by the enclosed material. More STM images of macrocycles are shown in Figure S2 in the Supporting Information.

To obtain larger, well ordered islands of chains, DMTP was deposited at a sample temperature of 440 K. The corresponding STM images are shown in Figure 5. Islands with aligned chains exceeding 200 × 200 nm^2 with defect-free areas of up to 60 × 60 nm^2 were observed. The complete absence of cyclic structures shows that islands of chains are thermodynamically more stable. While deposition of DMTP at room temperature led to vacancy islands in the top layer of the Cu(111) surface, these vacancy islands are not observed for the same coverage adsorbed at 440 K. Apparently, there is sufficient mobility and availability of Cu adatoms at this temperature.

Formation of long-range ordered structures requires reversible bond formation and scission, such that initial defects can heal. For the organometallic polymer chains, this restructuring process is slow on the time scale of the STM experiment at 300 K and could thus be monitored for selected sample areas. Figure 6 shows two time sequences: In Figure 6a−c, an island with an initial width of four chains (see the framed region in Figure 6a) first loses (Figure 6b) and then regains a chain (Figure 6c). Note that the upper-left end of the island in Figure 6a−c also changes with time. The hexagonal loop in Figure 6a,b indicates that one chain is back-folded, and the fuzzy zone around the end, which is especially visible in Figure 6c, likely consists of larger and therefore more mobile loops or open-ended chains (see the Discussion). The second sequence, Figure 6d−f, shows a row of five ring-like features between two islands (framed region). In Figure 6d, the three "rings" on the left are formed by chains continuing from island to another, while the ring on the right stems from a back-folded chain from the upper island. Rings number 2 and 3 (counted from the left) show enclosed features, which may be one or more terphenyl fragments. In the next frame, taken after 9 min (Figure 6e), ring number 3 collapsed, while the loop formed by the back-folding chain on the right has increased in size and contains a weak enclosed feature. Another 9 min later (Figure 6f), ring number three is restored without an enclosed bright feature; the two rings on the right have turned into a fuzzy area. These changes illustrate the reversible character of the bond formation as a prerequisite for the formation long-range ordered structures. It cannot be excluded that the tip has an additional minor influence, but the fact that ordered islands occur at room temperature indicates that the observed processes have at least partly spontaneous character.

DISCUSSION

Structural Aspects. Submonolayers of DMTP on Cu(111) at 300 K undergo spontaneous C−Br bond scission. The resulting *meta*-terphenyl fragments are linked by Cu atoms, which bind to the terminal C atoms, such that organometallic macrocycles with C−Cu−C bridges and chains with zigzag structure are formed. Related,

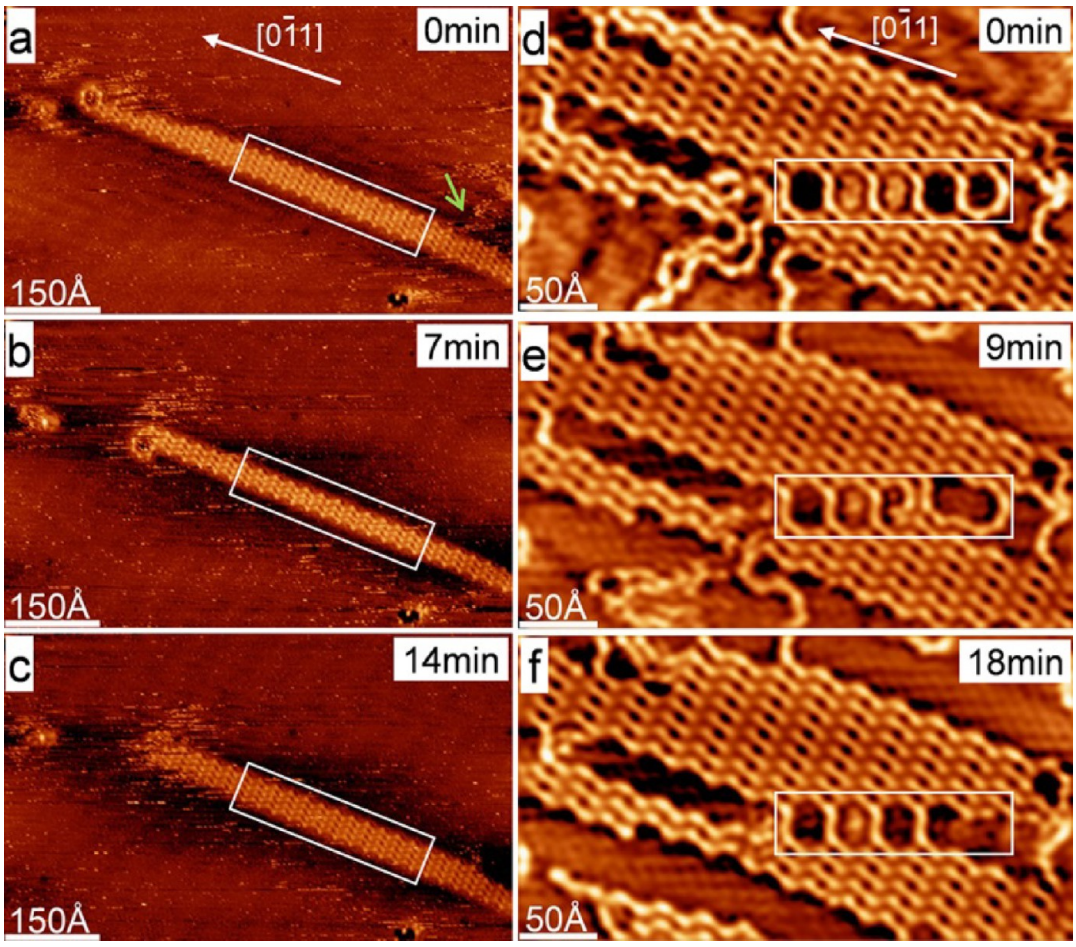

Figure 6. Two sequences of STM images of islands of species 2 obtained at 300 K. The image sequence (a–c) shows how an island first shrinks and then grows in width; $U = -2.75$ V, $I = 0.03$ nA. The sequence (d–f) shows the dissociation and formation of C–Cu–C bonds; $U = -2.75$ V, $I = 0.06$ nA. The green arrow in (a) marks the position where a chain appears to detach from the island.

but straight chains with C–Ag–C or C–Cu–C bonds have previously been reported.[19,27,28] The zigzag structure is caused by the bent geometry of the terphenyl units; this specific precursor geometry enables the formation of folded chains and macrocycles.

A model for the adsorption structure of the chains must be based on the following observations:

(1) The chains have angles of ±5.0° relative to the high symmetry directions of the substrate.

(2) The apparent height of the coordinated Cu atoms alternates, such that every other Cu atom along a chain appears brighter. Figure 2e shows line scans for two adjacent straight parts of a chain. The two curves deviate around a lateral distance value of 8 Å, which is the position of the Cu atoms.

These observations in combination with the unit cell dimensions provide tight restriction for the possible adsorbate structures. Furthermore, it is reasonable to assume that the Cu atoms in the C–Cu–C bridges prefer 3-fold hollow sites on the substrate, because these sites provide the highest possible coordination number and represent the positions which the atoms would occupy in an additional Cu layer.

On the basis of these considerations, a structural model for commensurate adsorption as shown in Figure 2d is proposed. If a randomly selected Cu atom of a chain (first atom) is placed on a 3-fold hollow site, the next Cu atom of this chain will sit on a bridge site. The following third Cu atom occupies an approximate 3-fold hollow site, while the fourth Cu atom occupies an on-top site. The fifth Cu atom finally has a position equivalent to that of the first Cu atom. This means that the length of the unit cell along the chains is doubled to 51.8 Å if the substrate is taken into account. This is in very good agreement to the doubled experimental unit cell length of 53.0 Å. Further details and an alternative structural model are presented in the Supporting Information (Figure S4).

Reactivity. At room temperature and at 440 K, DMTP on Cu(111) reacts exclusively to form species with C–Cu–C bonds, while C–C bond formation was not observed. This result gives insight into the mechanism of the C–Br bond scission: If bond scission would be induced by the (111) terrace alone and result in the formation of terphenyl fragments, one would expect that these formal biradicals combine with a certain

probability to form C−C bonds. The complete absence of this reaction suggests that Cu adatoms participate in the C−Br scission, such that a Br atom is directly replaced by a Cu atom without formation of an intermediate terphenyl biradical. Most likely, the Cu atoms for this reaction stem from the 2D adatom gas, making its rate of formation a matter of interest: The sum of the energy of formation of a Cu adatom on a Cu(111) terrace and its activation energy for diffusion is 0.78 ± 0.04 eV.[33] Since the diffusion activation energy is 37 ± 5 meV,[34] the energy of formation amounts to 0.74 eV. Under the reasonable assumption that there are no further activation barriers and using an estimated frequency factor of 10^{13} s^{-1}, the first-order reaction rate constant for adatom formation is 3.7 s^{-1} at 300 K. The formation of Cu adatoms is thus sufficiently fast on the time scale of our experiment, which proceeds over several minutes. (Note that the estimated frequency factor is justified by its closeness to the universal frequency factor from the Eyring equation,[35] k_BT/h, and to the diffusion frequency factor for Cu adatoms on Cu(111) of $5 \times 10^{13\pm1}$ s^{-1}.[34]) Despite a sufficient rate of formation of the Cu adatoms, their availability may be limited at higher coverages, when the step edges get increasingly blocked by chains (Figure 4a). In this situation, Cu atoms are pulled out from the terraces, such that vacancy islands of monatomic height are formed (Figure 3a). Consistent with this interpretation, there are more Cu atoms in C−Cu−C bridges than missing Cu atoms in vacancy islands. The precise ratio is 1.52 : 1, according to a statistical analysis of a large surface area (Figure S3a in the Supporting Information). The additional Cu atoms in the C−Cu−C bridges stem from step edges. The vacancy islands are rather uniform in size and have widths of approximately 50 Å (Figure 3c), which agrees with the lattice constant of the chain/surface system in the direction along the chains. This is possibly not a coincidence: Removal of Cu from the edge of a vacancy island and thus the growth of the vacancy island may come to a halt as soon as stable chains can grow on the bottom of the vacancy island, as shown by Figure S3b in the Supporting Information. A stable chain has a minimum length of one unit cell of the chain/surface system, which is 51.8 Å according to the model in Figure 2d.

Dynamics. Island growth of the chains can proceed by attachment of individual terphenyl units and Cu atoms, or alternatively, by attachment of an oligomer chain formed on a terrace. Similarly, islands can shrink by detachment of either single terphenyl units or complete chains. Even though the limited temporal resolution of our experiment (several minutes per image) did not allow us to directly observe the attachment/detachment events, the sequence in Figure 6a−c gives some insight into the growth dynamics of an island: First, the island loses a whole chain from Figure 6a to b and then regains a whole chain from Figure 6b to c, which suggests that preformed chains can attach or detach. Such isolated chains are probably responsible for the fuzzy appearance of the areas around the island, in which chains of different lengths and monomers diffuse rapidly on the time scale of the STM experiment.

Closer inspection of Figure 6a shows a feature that is probably a chain partly attached, and partly detached from an island: the green arrow marks the point at which the chain turns into a fuzzy region on the terrace, most likely a chain moving during STM imaging. Additional evidence for preformed chains attaching to islands is seen in Figure 4d, where a chain at the periphery of an island forms a loop. It is unlikely that such a loop is generated when the chain grows by attaching individual terphenyl units.

Notably, the island in Figure 6a−c does not grow in length in the sequence 6a → 6b → 6c. A possible explanation is the formation of loops, which results in backfolding of the chain and thus termination of the island. One such loop of minimal size (an approximate hexagon) and therefore maximum conformational rigidity can be seen at the left end of the island in Figure 6a,b. In Figure 6c, a fuzzy region occurs instead, which probably consists of loops with larger diameters and thus more conformational flexibility. That a loop can easily change its size by reacting with a neighboring chain is illustrated by the sequence in Figure 6d,e, where a hexagonal loop turns into a larger loop (which can be imaged here because it is stabilized by the surrounding chains).

These observations suggest the following mechanism for the island formation: after initial nucleation (*e.g.*, at a step edge), an island grows by addition of terphenyl units and Cu atoms, and by addition of preformed oligomer chains. The large aspect ratio of the island of up to 25:1 indicates that the start or addition of a new chain is slower than the growth of an existing chain, if only the kinetics of formation is considered. However, since the data in Figure 6a−c show that the attachment of preformed chains is reversible, it is more appropriate to state that the rate constant for the attachment of a chain is only slightly larger than the rate constant for the detachment of a chain. This is not surprising, because the energy needed for the detachment is partly compensated by the translational and configurational entropy gained by the detached chain. An island stops growing when it reaches another island or a step edge, or by formation of loops and backfolding of chains.

The observation that macrocycles appear at room temperature and below, whereas only chains are formed at elevated temperatures, indicates that the latter are thermodynamically favored. This can be explained with the high packing density that is reached when the chains form islands and that allows a maximum of lateral van der Waals interactions. In contrast,

the macrocycles have a lower packing density and a lower amount of attractive interactions per surface area and per repeat unit. If the chains are thermodynamically favored, then the formation of rings must either be kinetically favored, or they only appear as the minority species in a temperature-dependent equilibrium with the chains. Ring closure of an existing chain fragment is a first-order reaction and thus, at low coverages, kinetically favored over the bond formation between two chains or the attachment of another terphenyl fragment to an existing chain, which are second-order reactions. This fact has frequently been employed in solution chemistry, where high-dilution techniques are used to increase the yield in cyclization reactions.[36] From a thermodynamic point of view, the formation of rings may be more favorable at low temperatures; however, the availability of Cu adatoms may be the limiting factor then. On the basis of these considerations, strategies for maximizing the yield of the organometallic macrocycles can be developed.

CONCLUSIONS

4,4″-Dibromo-*meta*-terphenyl (DMTP) adsorbs dissociatively on Cu(111) at 300 K and above by C−Br bond scission. The resulting *meta*-terphenyl fragments form room-temperature stable organometallic macrocycles and polymer chains with C−Cu−C bonds. The chains have a zigzag structure, a repeat unit length of 26.5 Å, and extend in directions of ±5.0° relative to the high-symmetry direction of the Cu(111) substrate. A chain can bend by angles of 60° and 120° or backfold (180°). Islands formed by these chains are elongated along the chain direction. The coordinated Cu atoms along a chain show a periodic variation of the apparent height. This is explained with a structural model, in which the Cu atoms in the chain alternately occupy hollow, bridge and on-top sites. The Cu atoms in the C−Cu−C bonds stem partly from the terraces, as can be seen by the formation of vacancy islands at higher coverages. In addition to the polymer chains, cyclic oligomers of the type (*meta*-terphenyl-Cu)$_n$ with n = 6, 8, 14, 16, 18, 22 were observed. They are less stable than the chains, presumably because of their lower packing density, and represent possible intermediates in the surface-confined Ullmann synthesis of hydrocarbon macrocycles such as hyperbenzene. Deposition of DMTP at 440 K leads to larger islands of chains, but no cyclic structures occur. The fact that only C−Cu−C, but no C−C bond formation occurs at 300 and 440 K suggests that Cu adatoms participate in the C−Br bond scission, such that Br is directly replaced by Cu. Island growth can proceed both by attachment of monomers and complete oligomer chains; the detachment of chains has also been observed. Termination of islands often results from backfolding of chains, which prevents further growth in length. This study shows that the surface-assisted synthesis of organometallic oligomers and polymers with carbon−metal−carbon bonds can provide a variety of room-temperature stable linear and cyclic compounds, especially if the substrate symmetry is carefully matched to the symmetry of the organic linker. The resulting compounds can be used for the functionalization of surfaces or as intermediates for the synthesis of covalent nanostructures.

METHODS

The experiments were performed in a two-chamber UHV system, which has been described previously,[37] at a background pressure below 10^{-10} mbar. The scanning tunneling microscope is a SPECS STM 150 Aarhus with SPECS 260 electronics. All voltages refer to the sample and the images were recorded in constant current mode. Moderate filtering (Gaussian smooth, background subtraction) has been applied for noise reduction. The Cu(111) single crystal with an alignment of better than 0.1° relative to the nominal orientation was purchased from MaTecK, Germany. Preparation of a clean and structurally well controlled Cu(111) surface was achieved by cycles of bombardment with Ar^+ ions and annealing at 850 K. As described elsewhere,[22] 4,4″-dibromo-1,1′:3′,1″-terphenyl (4,4″-dibromo-*meta*-terphenyl, DMTP) was made from 4-bromophenylacetylene in a short reaction sequence utilizing a Grubbs-enyne metathesis reaction and a regioselective cobalt-catalyzed Diels−Alder reaction followed by mild oxidation. DMTP was vapor-deposited from a home-built Knudsen cell evaporator with a Ta crucible held at 360 K. STM images were recorded at a sample temperature of 300 K or at the indicated temperatures. XPS was performed with a VG MARK II spectrometer using a Mg Kα X-ray source (1253.6 eV). All binding energies were referenced to the Fermi edge of clean Cu ($E_b \equiv 0$). Unless otherwise indicated, the photoelectrons were detected at 60° to the surface normal for increased surface sensitivity. The deposition rate of DMTP was 0.11 ML/min unless indicated otherwise. Coverages were derived from STM images. The coverage of 1 ML refers to a densely packed layer of chains **2** and equals 0.040 DMTP molecules per surface copper atom.

Conflict of Interest: The authors declare no competing financial interest.

Acknowledgment. J.F.Z. acknowledges the financial support from the National Basic Research Program of China (2010CB923302, 2013CB834605), the National Natural Science Foundation of China (Grant No.21173200), and the Specialized Research Fund for the Doctoral Program of Higher Education of Ministry of Education (Grant No. 20113402110029). J.M.G. thanks the Deutsche Forschungsgemeinschaft for support through SFB 1083 and the Chinese Academy of Sciences for a Visiting Professorship for Senior International Scientists (Grant No. 2011T2J33).

Supporting Information Available: X-ray photoelectron spectra; additional STM images of organometallic macrocycles; STM image of a vacancy island; details of the structural model and alternative adsorption model of organometallic chains; role of the Br atoms. This material is available free of charge *via* the Internet at http://pubs.acs.org.

REFERENCES AND NOTES

1. Barth, J. V.; Costantini, G.; Kern, K. Engineering Atomic and Molecular Nanostructures at Surfaces. *Nature* **2005**, *437*, 671–679.
2. Lee, J.; Farha, O. K.; Roberts, J.; Scheidt, K. A.; Nguyen, S. T.; Hupp, J. T. Metal-Organic Framework Materials as Catalysts. *Chem. Soc. Rev.* **2009**, *38*, 1450–1459.

3. Murray, L. J.; Dinca, M.; Long, J. R. Hydrogen Storage in Metal-Organic Frameworks. *Chem. Soc. Rev.* **2009**, *38*, 1294–1314.
4. Kurmoo, M. Magnetic Metal-Organic Frameworks. *Chem. Soc. Rev.* **2009**, *38*, 1353–1379.
5. Heim, D.; Ecija, D.; Seutert, K.; Auwärter, W.; Aurisicchio, C.; Fabbro, C.; Bonifazi, D.; Barth, J. V. Self-Assembly of Flexible One-Dimensional Coordination Polymers on Metal Surfaces. *J. Am. Chem. Soc.* **2010**, *132*, 6783–6790.
6. Haq, S.; Hanke, F.; Dyer, M. S.; Persson, M.; Iavicoli, P.; Amabilino, D. B.; Raval, R. Clean Coupling of Unfunctionalized Porphyrins at Surfaces To Give Highly Oriented Organometallic Oligomers. *J. Am. Chem. Soc.* **2011**, *133*, 12031–12039.
7. Shi, Z.; Lin, N. Porphyrin-Based Two-Dimensional Coordination Kagome Lattice Self-Assembled on a Au(111) Surface. *J. Am. Chem. Soc.* **2009**, *131*, 5376–5377.
8. Wang, L.; Kong, H.; Chen, X.; Du, X.; Chen, F.; Liu, X.; Wang, H. Conformation-Induced Self-Assembly of Rubrene on Au(111) Surface. *Appl. Phys. Lett.* **2009**, *95*, 093102–1−093102−3.
9. Buchner, F.; Flechtner, K.; Bai, Y.; Zillner, E.; Kellner, I.; Steinrück, H.-P.; Marbach, H.; Gottfried, J. M. Coordination of Iron Atoms by Tetraphenylporphyrin Monolayers and Multilayers on Ag(111) and Formation of Iron-Tetraphenylporphyrin. *J. Phys. Chem. C* **2008**, *112*, 15458–15465.
10. Barth, J. V.; Weckesser, J.; Trimarchi, G.; Vladimirova, M.; De Vita, A.; Cai, C. Z.; Brune, H.; Gunter, P.; Kern, K. Stereochemical Effects in Supramolecular Self-Assembly at Surfaces: 1-D *versus* 2-D Enantiomorphic Ordering for PVBA and PEBA on Ag(111). *J. Am. Chem. Soc.* **2002**, *124*, 7991–8000.
11. Gourdon, A. On-Surface Covalent Coupling in Ultrahigh Vacuum. *Angew. Chem., Int. Ed.* **2008**, *47*, 6950–6953.
12. Shi, Z.; Lin, N. Structural and Chemical Control in Assembly of Multicomponent Metal-Organic Coordination Networks on a Surface. *J. Am. Chem. Soc.* **2010**, *132*, 10756–10761.
13. Li, Y.; Xiao, J.; Shubina, T. E.; Chen, M.; Shi, Z.; Schmid, M.; Steinrück, H.-P.; Gottfried, J. M.; Lin, N. Coordination and Metalation Bifunctionality of Cu with 5,10,15,20-Tetra(4-pyridyl)porphyrin: Toward a Mixed-Valence Two-Dimensional Coordination Network. *J. Am. Chem. Soc.* **2012**, *134*, 6401–6408.
14. Lin, N.; Dmitriev, A.; Weckesser, J.; Barth, J. V.; Kern, K. Real-Time Single-Molecule Imaging of the Formation and Dynamics of Coordination Compounds. *Angew. Chem., Int. Ed.* **2002**, *41*, 4779–4783.
15. Gambardella, P.; Stepanow, S.; Dmitriev, A.; Honolka, J.; de Groot, F. M. F.; Lingenfelder, M.; Sen Gupta, S.; Sarma, D. D.; Bencok, P.; Stanescu, S.; *et al.* Supramolecular Control of the Magnetic Anisotropy in Two-Dimensional High-Spin Fe Arrays at a Metal Interface. *Nat. Mater.* **2009**, *8*, 189–193.
16. Stepanow, S.; Lin, N.; Payer, D.; Schlickum, U.; Klappenberger, F.; Zoppellaro, G.; Ruben, M.; Brune, H.; Barth, J. V.; Kern, K. Surface-Assisted Assembly of 2D Metal-Organic Networks that Exhibit Unusual Threefold Coordination Symmetry. *Angew. Chem., Int. Ed.* **2007**, *46*, 710–713.
17. Ullmann, F.; Bielecki, J. Synthesis in the Biphenyl Series. *Ber. Deutsch. Chem. Ges.* **1901**, *34*, 2174–2185.
18. Di Giovannantonio, M.; El Garah, M.; Lipton-Duffin, J.; Meunier, V.; Cardenas, L.; Fagot Revurat, Y.; Cossaro, A.; Verdini, A.; Perepichka, D. F.; Rosei, F.; *et al.* Insight into Organometallic Intermediate and Its Evolution to Covalent Bonding in Surface-Confined Ullmann Polymerization. *ACS Nano* **2013**, *7*, 8190–8198.
19. Wang, W. H.; Shi, X. Q.; Wang, S. Y.; Van Hove, M. A.; Lin, N. Single-Molecule Resolution of an Organometallic Intermediate in a Surface-Supported Ullmann Coupling Reaction. *J. Am. Chem. Soc.* **2011**, *133*, 13264–13267.
20. Walch, H.; Gutzler, R.; Sirtl, T.; Eder, G.; Lackinger, M. Material- and Orientation-Dependent Reactivity for Heterogeneously Catalyzed Carbon-Bromine Bond Homolysis. *J. Phys. Chem. C* **2010**, *114*, 12604–12609.
21. Blunt, M. O.; Russell, J. C.; Champness, N. R.; Beton, P. H. Templating Molecular Adsorption Using a Covalent Organic Framework. *Chem. Commun.* **2010**, *46*, 7157–7159.
22. Fan, Q.; Wang, C.; Han, Y.; Zhu, J. F.; Hieringer, W.; Kuttner, J.; Hilt, G.; Gottfried, J. M. Surface-Assisted Organic Synthesis of Hyperbenzene Nanotroughs. *Angew. Chem., Int. Ed.* **2013**, *52*, 4668–4672.
23. Grill, L.; Dyer, M.; Lafferentz, L.; Persson, M.; Peters, M. V.; Hecht, S. Nano-Architectures by Covalent Assembly of Molecular Building Blocks. *Nat. Nanotechnol.* **2007**, *2*, 687–691.
24. Tait, S. L.; Langner, A.; Lin, N.; Stepanow, S.; Rajadurai, C.; Ruben, M.; Kern, K. One-Dimensional Self-Assembled Molecular Chains on Cu(100): Interplay Between Surface-Assisted Coordination Chemistry and Substrate Commensurability. *J. Phys. Chem. C* **2007**, *111*, 10982–10987.
25. Klappenberger, F.; Weber-Bargioni, A.; Auwärter, W.; Marschall, M.; Schiffrin, A.; Barth, J. V. Temperature Dependence of Conformation, Chemical State, and Metal-Directed Assembly of Tetrapyridyl-Porphyrin on Cu(111). *J. Chem. Phys.* **2008**, *129*, 214702–1−214702−10.
26. Classen, T.; Fratesi, G.; Costantini, G.; Fabris, S.; Stadler, F. L.; Kim, C.; de Gironcoli, S.; Baroni, S.; Kern, K. Templated Growth of Metal-Organic Coordination Chains at Surfaces. *Angew. Chem., Int. Ed.* **2005**, *44*, 6142–6145.
27. Park, J.; Kim, K. Y.; Chung, K.-H.; Yoon, J. K.; Kim, H.; Han, S.; Kahng, S.-J. Interchain Interactions Mediated by Br Adsorbates in Arrays of Metal-Organic Hybrid Chains on Ag(111). *J. Phys. Chem. C* **2011**, *115*, 14834–14838.
28. Chung, K.-H.; Koo, B.-G.; Kim, H.; Yoon, J. K.; Kim, J.-H.; Kwon, Y.-K.; Kahng, S.-J. Electronic Structures of One-Dimensional Metal-Molecule Hybrid Chains Studied Using Scanning Tunneling Microscopy and Density Functional Theory. *Phys. Chem. Chem. Phys.* **2012**, *14*, 7304–7308.
29. Villagomez, C. J.; Sasaki, T.; Tour, J. M.; Grill, L. Bottom-up Assembly of Molecular Wagons on a Surface. *J. Am. Chem. Soc.* **2010**, *132*, 16848–16854.
30. Hanke, F.; Haq, S.; Raval, R.; Persson, M. Heat-to-Connect: Surface Commensurability Directs Organometallic One-Dimensional Self-Assembly. *ACS Nano* **2011**, *5*, 9093–9103.
31. Xi, M.; Bent, B. E. Mechanisms of The Ullmann Coupling Reaction in Adsorbed Monolayers. *J. Am. Chem. Soc.* **1993**, *115*, 7426–7433.
32. Yoon, J. K.; Jung, G. E.; Kim, H.; Chung, K. H.; Kahng, S. J. Two-Dimensional Vacancy Islands Induced by the Growth of Cr on Cu(111). *Thin Solid Films* **2010**, *519*, 1375–1379.
33. Icking-Konert, G. S.; Giesen, M.; Ibach, H. Decay of Cu Adatom Islands on Cu(111). *Surf. Sci.* **1998**, *398*, 37–48.
34. Repp, J.; Moresco, F.; Meyer, G.; Rieder, K. H.; Hyldgaard, P.; Persson, M. Substrate Mediated Long-Range Oscillatory Interaction Between Adatoms: Cu/Cu(111). *Phys. Rev. Lett.* **2000**, *85*, 2981–2984.
35. Eyring, H. The Activated Complex in Chemical Reactions. *J. Chem. Phys.* **1935**, *3*, 107.
36. L. Rossa, F. V. Synthesis of Medio- and Macrocyclic Compounds by High Dilution Principle Techniques. In *Cyclophanes I, Topics in Current Chemistry*; Vögtle, F., Ed.; Springer: Berlin, Heidelberg, 2013; Vol. 113, p 1.
37. Chen, M.; Feng, X.; Zhang, L.; Ju, H.; Xu, Q.; Zhu, J. F.; Gottfried, J. M.; Ibrahim, K.; Qian, H.; Wang, J. Direct Synthesis of Nickel(II) Tetraphenylporphyrin and Its Interaction with a Au(111) Surface: A Comprehensive Study. *J. Phys. Chem. C* **2010**, *114*, 9908–9916.